

Article

The Effects of Carbon–Silica Dual-Phase Filler on the Crosslink Structure of Natural Rubber

Jingyi Wang^{1,2,*}  and Hongbing Jia^{2,*}

¹ School of New Materials and Shoes & Clothing Engineering, Liming Vocational University, Quanzhou 362000, China

² Key Laboratory for Soft Chemistry and Functional Materials of Ministry of Education, Nanjing University of Science and Technology, Nanjing 210094, China

* Correspondence: jingleewong@gmail.com (J.W.); polymernjust@gmail.com (H.J.)

Abstract: Carbon–silica dual-phase filler (CSDPF)/natural rubber (NR) vulcanizate was prepared by mechanical blending, followed by a hot-press vulcanization. The dispersion of CSDPF in the NR matrix and the effects of CSDPF on the filler–rubber interaction and structure of the rubber network were studied. Scanning electron microscope results showed that CSDPF dispersed uniformly; however, there were some aggregates of CSDPF when loading too many fillers. With an increase in CSDPF, the interaction between CSDPF and NR chains increases, which was detected by bound rubber in the CSDPF/NR compound. The spectra of solid-state nuclear magnetic resonance revealed that CSDPF could promote the formation of poly-sulfidic crosslink in the rubber vulcanization network. Further, the molecular chain movement ability of vulcanizates decreases according to the spin–spin relaxation of ¹H nuclei in CSDPF/NR compounds. The crosslink density of vulcanizate increases, while the chemical crosslink and physical crosslink in the vulcanization network also increase according to the tube model.

Keywords: natural rubber; filler; CSDPF; vulcanization; network structure



Citation: Wang, J.; Jia, H. The Effects of Carbon–Silica Dual-Phase Filler on the Crosslink Structure of Natural Rubber. *Polymers* **2022**, *14*, 3897. <https://doi.org/10.3390/polym14183897>

Academic Editor: Marcin Maslowski

Received: 24 August 2022

Accepted: 14 September 2022

Published: 18 September 2022

Publisher's Note: MDPI stays neutral with regard to jurisdictional claims in published maps and institutional affiliations.



Copyright: © 2022 by the authors. Licensee MDPI, Basel, Switzerland. This article is an open access article distributed under the terms and conditions of the Creative Commons Attribution (CC BY) license (<https://creativecommons.org/licenses/by/4.0/>).

1. Introduction

In rubber composites, carbon black and silica are the most used fillers. For carbon black, it can effectively improve the tensile strength, tearing strength and wear resistance of the rubber material; however, it causes high friction of rubber material. In the case of silica, it can significantly reduce friction and rolling resistance of rubber material; nevertheless, the mechanical strength of silica-filled rubber should be further improved. Thus, these two kinds of fillers were often filled into rubber together in practical applications [1]. Nevertheless, because the two fillers have different surface energy and poor compatibility, they cannot form a uniform filler network in rubber materials [2], which has limitations on the improvement of rubber.

Carbon–silica dual-phase filler (CSDPF) is a kind of hybrid filler and different from the physical mixing of carbon black and silica. CSDPF is prepared through symbiosis technology in the production process of carbon black, in which the carbon black is chemically modified by organic–silicon compounds. As a result, CSDPF exhibits two kinds of phase structure, which are the carbon black phase and silica phase. In other words, carbon black and silica are doped with each other, which effectively reduces the filler–filler interaction and improves their dispersion in the rubber matrix. Wang et al. [3,4] reported a series of works about CSDPF-filled rubber, but they focused on dynamic mechanical properties, and did not systematically study the static mechanical properties, filler–rubber interaction and rubber network structure.

Vulcanization is an important process, in which the crosslink network of rubber is formed. It is known that the crosslink network significantly affects the macro-properties of the rubber. In this work, CSDPF/natural rubber (NR) vulcanizate was prepared, and the

interaction between CSDPF and rubber was studied. Four methods of crosslink density, tube model, ^{13}C -NMR and ^1H -NMR were used to analyze the influence of CSDPF on the network structure of NR vulcanization.

2. Materials and Methods

2.1. Materials

CSDPF2125 (Si contained is 5.1 wt.%) was purchased from Cabot China Ltd., Shanghai. NR (RSS1) and the rest of the materials were provided by Nanjing JinSanLi Rubber & Plastic Co., Ltd., Nanjing, China.

2.2. Preparation of Composites

The formulation of the NR compound is summarized in Table 1. All ingredients were mixed in an LN-120 open two-roll mill (LINA machinery Industrial Co., Ltd., Dongguan China) at room temperature. The vulcanizates were prepared by a molding the above compounds at 143 °C and 15 MPa for the optimum cure time (t_{90}).

Table 1. Formulation of the CSDPF/NR compounds.

Sample	Constituent (Phr, Per Hundred Rubber)	
	CSDPF	NR
C0	0	100
C10	10	100
C20	20	100
C30	30	100
C40	40	100
C50	50	100

Other agents: ZnO 4, Stearic acid 2.5, Antioxidant RD 2.0, Coumarone indene resin 3, sulfur 2.0, accelerator NS 1.5.

2.3. Characterization

The bound rubber of compounds was determined according to Ref. [5].

$$\text{Bound rubber} = \frac{\omega_3 - \omega_2 - \omega_1 \frac{m_1}{m_1 + m_r}}{\omega_1 \frac{m_r}{m_1 + m_r} \cdot \omega_1 \frac{m_1}{m_1 + m_r}} \times 100 \quad (1)$$

where ω_1 , ω_2 and ω_3 are the weight of rubber before swelling, filler and the weight of rubber after drying, respectively. m_1 and m_r are the fraction of filler and rubber in the compound, respectively.

The tensile tests were measured on a universal testing machine (Shenzhen SANS Co., Ltd., Shenzhen, China) at a crosshead speed of 10 mm/min according to ASTM D412. The results were averaged based on five measurements.

The crosslink densities of the composites determined according to Ref. [5]. The samples were cut into rectangles ($10 \times 10 \times 2 \text{ mm}^3$) and weighed before and after being soaked in toluene for 7 days, which ensured a swelling equilibrium. The crosslink density (XLD) was calculated according to

$$\text{XLD} = - \frac{\ln(1 - \phi_r) + \phi_r + \chi_1 \phi_r^2}{\phi_r \left(\phi_r^{\frac{1}{3}} - \phi_r / 2 \right)} \quad (2)$$

$$\phi_r = \frac{\frac{\omega_1}{\rho_d}}{\frac{n_2 - n_1}{\rho_s} + \frac{n_1}{\rho_d}} \quad (3)$$

where n_1 and n_2 are the mass of sample before swelling and swollen, respectively. The ρ_d is the density of the sample before swelling and ρ_s is the toluene density (0.8669 g/mL). χ_1 is the Flory–Huggins interaction parameter between toluene and rubber (0.391).

The freeze-fracture surface morphology of the samples was observed with a JSM-6700F scanning electron microscope (SEM, JEOL Ltd., Akishima, Japan).

Solid-state nuclear magnetic resonance (NMR) spectroscopy was performed with a Bruker Avance III NMR spectrometer (Bruker Corporation, Billerica, MA, USA) operating at 400 MHz and 100 MHz for ^1H and ^{13}C , respectively. The magic-angle spin (MAS) rate of the sample tube for the NMR measurement was 10 kHz. The spectra were recorded from a single-pulse experiment using high-power decoupling. The $\pi/2$ pulse width for ^{13}C was 6 μs with a 3 μs width decoupling pulse for ^1H . The number of scans for acquisition of spectra was 30 k. The spin–spin relaxation time (T_2) were measured by the Carr–Purcell–Meiboom–Gill (CPMG) method.

3. Results

3.1. Dispersion of CSDPF

Figure 1 shows the fracture surfaces of CSDPF/NR vulcanizates. As can be seen in Figure 1a, CSDPF is evenly dispersed in the NR matrix when the filling amount is less; the larger-size CSDPF is shown on the fracture surface when the loading is increased to 50 phr (Figure 1c). Due to the high surface area (171 m^2/g) of CSDPF, NR chains are adsorbed strongly onto CSDPF's surface. Thus, high surface area and high loading of filler used in NR induce small distances between reinforcing fillers so that almost any rubber chain contacts at least one filler aggregate [6]. In addition, because the statistical size of polymeric chains is in the range of interaggregate distances, close-neighboring objects are probably bound together by chains adsorbed onto both aggregates. Therefore, the larger-size filler is present in SEM.

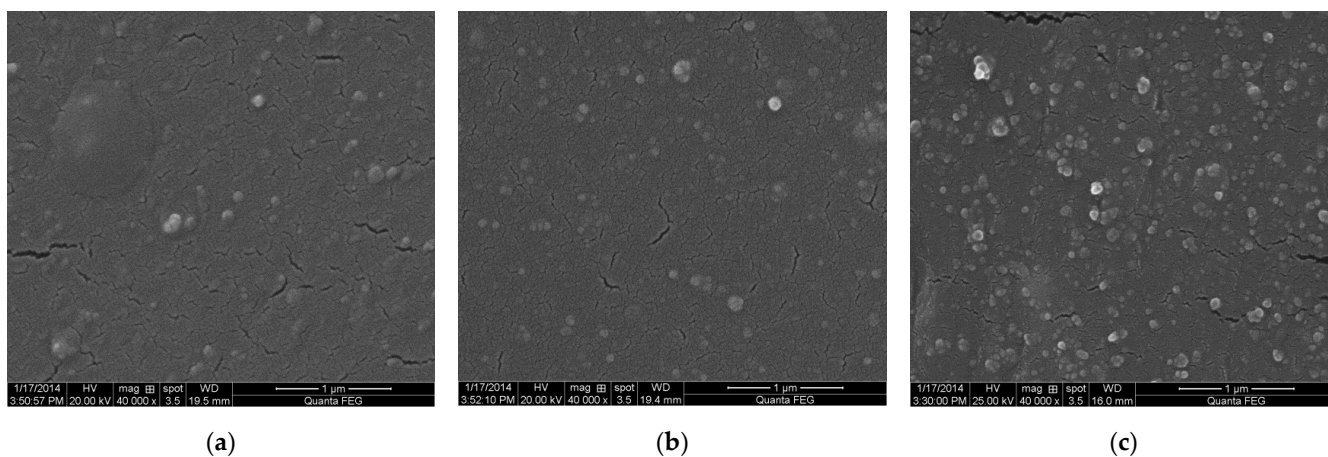


Figure 1. SEM images of freeze-fractured surface of CSDPF/NR vulcanizates, (a) C10, (b) C30 and (c) C50.

In order to further understand the structure of filler network, bound rubber (BdR) of CSDPF/NR compound was measured and is shown in Figure 2a. Bound rubber is a part of rubber that cannot be extracted by a good solvent. From the phenomenological point of view, the bound rubber can be understood as a part of the rubber that the filler particles form into a three-dimensional reticular formation in rubber to adsorb or encapsulate in rubber [7]. Therefore, as seen in Figure 2a, the BdR increases gradually and reaches the maximum when loading 30 phr of CSDPF. When the content of filler is low, the discrete CSDPF adsorbed a certain number of NR chain segments (such as Figure 2a illustrates). With an increase in filler, the CSDPF aggregates begin to approach each other; therefore, in addition to the NR chain segments adsorbed on the surface of the CSDPF aggregate, there are other NR chains entangled between the adjacent CSDPF aggregates. As a consequence, the BdR increases. As the amount of filler is further increased to 30 phr, more and more NR chain segments are entangled between adjacent CSDPF aggregates and there are even NR chain segments trapped between CSDPF aggregates [2,8]; thus, the BdR reaches its peak.

However, when more fillers are added, the CSDPF aggregates form an agglomeration; thus, the NR segment of the adsorbed was reduced (graph embedded in Figure 2a), causing a reduction in BdR.

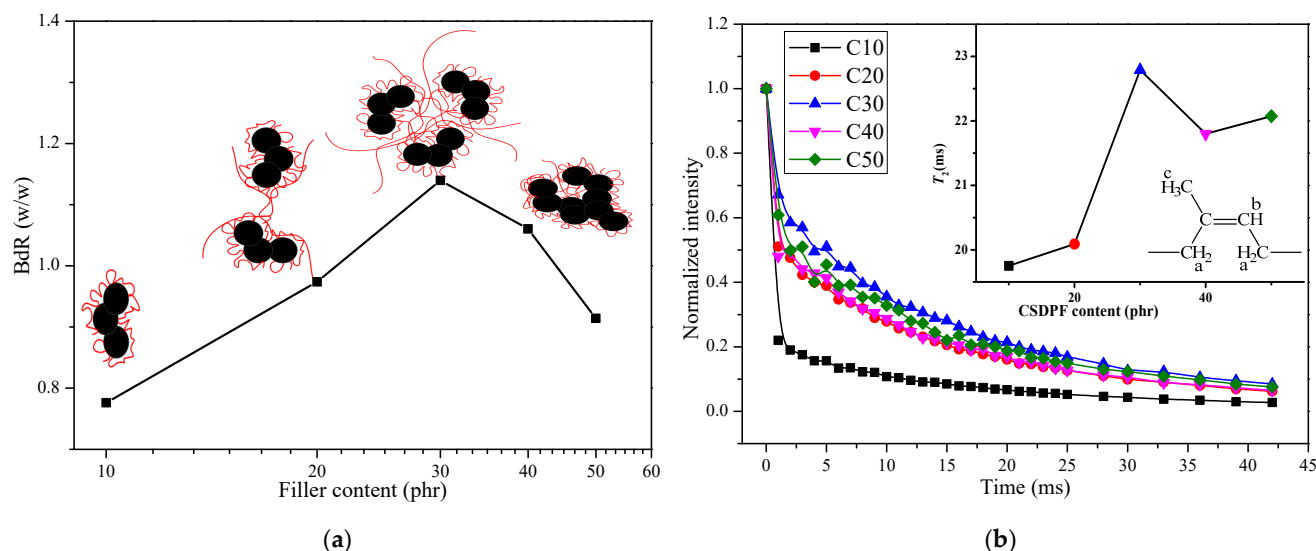


Figure 2. (a) BdR of CSDPF/NR compounds, (b) Spin–spin relaxation and T_2 of Hb nuclei (inset image) in bound rubber.

Figure 2b shows the spin–spin relaxation and the contact time T_2 of Hb protons in CSDPF/NR vulcanizates. T_2 reflects the movement of all molecules in the entire rubber network, including information of fast motion and slow motion [9]. It can be seen in Figure 2b that the T_2 of the Hb protons in bound rubber increases with the addition of CSDPF, and reaches a maximum value when adding 30 phr of CSDPF. This is consistent with the trend of BdR. Because BdR increases gradually with an increase in the amount of filler; that is, the number of rubber chain segments adsorbed by each filler increases. As a result, the effect of each filler on the molecule movement of the whole rubber network of bound rubber is gradually reduced; thus, the T_2 increases.

3.2. Crosslink Structure of Vulcanization Network

Figure 3a is a crosslink density (XLD) diagram of CSDPF/NR vulcanizate. It can be seen that the XLD of the vulcanizate drops when a small amount of CSDPF is added. This is due to the adsorption of accelerators on the silica phase on CSDPF, which leads to a decrease in the crosslink degree of the vulcanizate [4,10]. The XLD of the vulcanizate increases with the further addition of CSDPF. On the one hand, due to the addition of more CSDPF, the interaction between silica phases on the CSDPF surface reduced the adsorption of accelerant to a certain extent; that is, it promoted an increase in crosslink degree of vulcanizate; on the other hand, the calculation of XLD is based on the Flory–Rehner swelling model: the smaller the swelling degree of the vulcanizate is, the greater the XLD is, but, in the calculation of the swelling model, only the volume of the filler is simply deducted, and the effect of the filler–rubber interaction on the swelling volume is not taken into account [11].

In order to study the effect of CSDPF on the vulcanization crosslinking point of natural rubber vulcanizate, the solid-state ^{13}C -NMR was used. Figure 3b shows a ^{13}C -NMR diagram of typical natural rubber vulcanizate; Figure 3c is a ^{13}C -NMR diagram of different CSDPF/NR in the 10–70 ppm region. In Figure 3b, there are five major nuclear magnetic signals that correspond to five different carbon atoms on the NR molecular chain (inset image). In Figure 3c, there are four smaller signals, and their chemical shifts are 44.1, 44.7, 50.4 and 58.0 ppm, respectively. Among them, the chemical shift of 44.7 ppm corresponds to the mono-sulfidic crosslink in the crosslinked bond, and the signals of 44.1, 50.4 and

58.0 ppm correspond to the poly-sulfidic crosslink in the crosslinked bond, respectively [12]. The signal (C5, 24.0 ppm) of methyl carbon was selected to normalize the four smaller signal intensities:

$$\chi_{Xp.p.m.} = \frac{I_{Xp.p.m.}}{I_{24.0p.p.m.}} \tag{4}$$

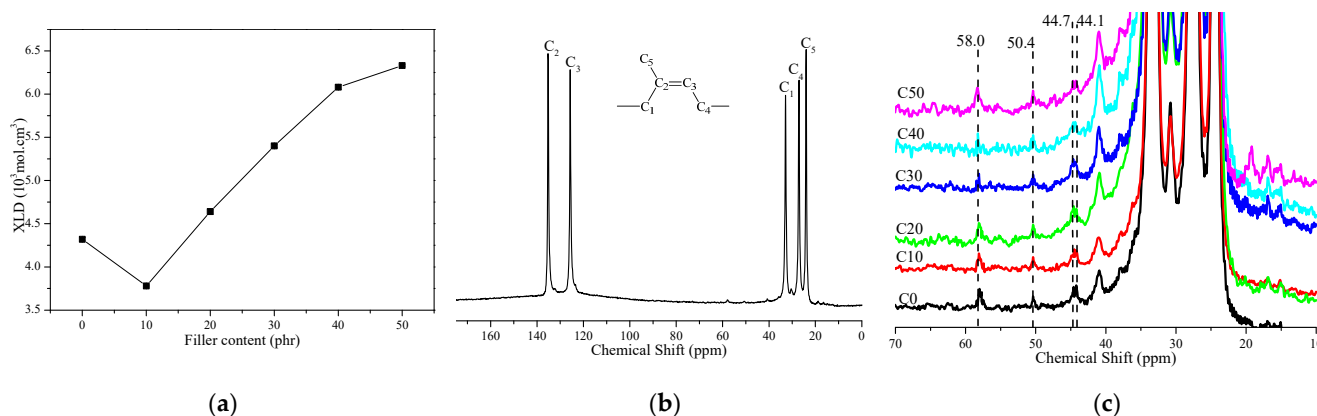


Figure 3. (a) Crosslink density (XLD), (b) full region of ¹³C-NMR spectra and (c) region from 70–10 ppm of ¹³C-NMR spectra of CSDPF/NR vulcanizates.

Among them, χ represents the chemical shift of the corresponding signal peak, and I is the intensity of the corresponding signal peak. The results are brought into the next formula and the content distribution of the mono-sulfidic crosslink and poly-sulfidic crosslink is calculated:

$$A_Y(\%) = \frac{\chi_Y}{\chi_{mono} + \chi_{poly}} \times 100 \tag{5}$$

Among which, Y is the type of crosslinked bond and χ is the relative intensity of the signal of the corresponding crosslinked bond after normalization. The results are listed in Table 2. It can be seen that the content of the poly-sulfidic crosslink of C10 increases from 72.8% to 74.1%. In the vulcanization process, the content of the poly-sulfide bond is proportional to the ratio of sulfur/accelerator [12]. The silica phase on CSDPF will adsorb accelerators [4,10] and reduce the content of accelerators. Thus, the ratio of sulfur/accelerator is increased and, finally, the content of the poly-sulfidic crosslink in C10 is increased. With the further addition of CSDPF, the interaction between silica phases on the CSDPF surface reduces the adsorption of accelerators. As a result, the ratio of sulfur/accelerator decreases, causing a reduction in the content of the poly-sulfidic crosslink.

Table 2. ¹³C-NMR data of CSDPF/NR vulcanizates.

Sample		C0	C10	C20	C30	C40	C50	
Signal-to-noise ratio		1105	1009	1053	1130	1081	981	
Relative intensity of signals ($\times 100$)	Mono-sulfidic crosslink	44.7 ppm	3.5	2.1	3.6	2.1	2.4	3.6
	Poly-sulfidic crosslink	44.1 ppm	3.5	2.3	3.8	2.3	2.6	3.5
		50.4 ppm	3.1	2.2	3.2	1.8	2.1	3.2
		58.0 ppm	2.8	1.7	2.9	1.6	1.8	3.5
Mono-sulfidic crosslink (%)		27.2	25.9	26.9	27.3	27.0	26.0	
Poly-sulfidic crosslink (%)		72.8	74.1	73.1	72.7	73.0	74.0	

3.3. Network Structure of CSDPF/NR

The network structure of rubber includes chemical crosslink and physical crosslink, which play an important role in the mechanical properties of rubber. In this section, a

tensile test performed at low strain rate, i.e., 10 mm/min, was utilized in the tube model analyses. The relevant equations are as follows [13]:

$$\sigma_M(\lambda') = \frac{\sigma}{(\lambda' - \lambda'^{-2})} = G_c(\varphi) + G_e(\varphi)f(\lambda') \tag{6}$$

$$f(\lambda') = 2\left(\frac{\lambda'^{0.5} - \lambda'^{-1}}{\lambda'^{1/2} - \lambda'^{-1}}\right), \lambda' \neq 1 \tag{7}$$

$$f(\lambda') = 1, \lambda' = 1 \tag{8}$$

$$\lambda' = (\lambda - 1)E/E_0 + 1 \tag{9}$$

Among them, σ_M is the Mooney stress, σ is the actual stress, λ' is the internal strain rate, φ is the volume fraction of the filler, G_c is the contribution of the chemical crosslink to the elastic modulus, G_e is the contribution of the physical crosslink to the elastic modulus, λ is the macro-strain ratio and $f(\lambda)$ is the strain equation. E and E_0 are the initial elastic modulus of vulcanizate with fillers and no fillers, respectively.

Figure 4 is a σ_M - $f(\lambda')$ diagram of CSDPF/NR vulcanizates with different contents of filler. It can be seen that under low strain (high $f(\lambda')$), the σ_M of all samples falls sharply, which is attributed to the Payne effect [11,14]. Under low strain, the network structure of the filler aggregates is destroyed, resulting in a significant reduction in the modulus of the vulcanizate; that is, there is a sharp decrease in σ_M . However, under high strain (low $f(\lambda')$), σ_M of the samples shows a trend of increasing sharply; this is due to the tensile-induced crystallization of NR under high strain [15,16]. However, the trend is slow with the increase in CSDPF. This is attributed to the decrease in crystallization properties of NR with presence of filler [17].

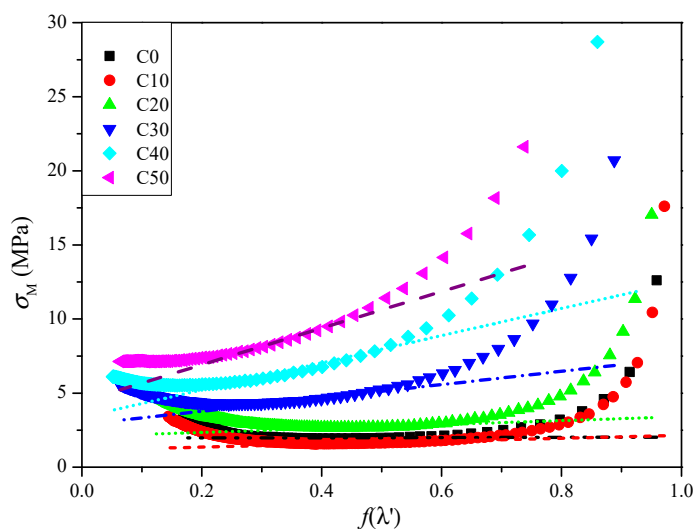


Figure 4. σ_M - $f(\lambda')$ curves of CSDPF/NR vulcanizates.

In the middle area of Figure 4, the tangent line is cut along the flat area of the curve; the tangent intercept and the slope obtained correspond to the G_c and G_e of the vulcanizate, respectively. The results are listed in Table 3. It can be seen that the G_c of the C10 sample is reduced and the G_e increases upon adding a small amount of CSDPF. Compared with the unfilled vulcanizate (C0), it seems that the chemical crosslink part decreases in the vulcanization network of the C10 sample and the physical crosslink part increases. As mentioned above, the silica phase on the surface of CSDPF will adsorb the accelerators and reduce the degree of chemical crosslink of the rubber, so the G_c of the vulcanizate is reduced. The rubber chain is entangled on the surface of CSDPF, which is the physical adsorption in bound rubber, and forms physical crosslinks [18]. Consequently, the G_e of vulcanizate increases. As the filler increases, both the G_c and G_e of the CSDPF/NR

vulcanizates are increased. For G_c , on the one hand, more CSDPF causes greater interaction between the silica phases of CSDPF, and reduces the adsorption of accelerators to a certain extent. On the other hand, the chemical crosslink formed by the active point of filler and rubber segments [19] increases gradually, eventually leading to an increase in G_c . For the G_e , as the CSDPF increases, not only do the rubber chain segments adsorbed on the CSDPF surface increase, but the rubber segments will also be trapped in the CSDPF aggregates (inset image in Figure 2a). Therefore, G_e increases.

Table 3. Parameters of network in CSDPF/NR vulcanizates.

Sample	G_c (MPa)	G_e (MPa)	$G_c + G_e$ (MPa)	$1/T_2^{XL}$ (10^{-2} ms^{-1})	XLD ($10^4 \text{ mol}\cdot\text{cm}^{-3}$)
C0	2.0	0.7	2.7	4.73	4.32
C10	1.2	1.0	2.2	5.36	3.78
C20	2.1	1.3	3.4	5.87	4.64
C30	2.9	4.5	7.4	6.38	5.40
C40	3.4	9.2	12.6	6.57	6.08
C50	4.4	12.4	16.8	7.21	6.33

The total crosslink network $G_c + G_e$ obtained by the tube model and the data $1/T_2^{XL}$ obtained by NMR are further compared with the XLD obtained by the swelling method; the data are listed in Table 3. Because the spin–spin relaxation time of NMR is inversely proportional to the crosslink density [20,21], the crosslink density of NMR method is replaced by $1/T_2^{XL}$, accordingly. It can be seen that with the increase in filler, the trend of the crosslink network obtained by the tube model is consistent with that of the crosslink density obtained by the swelling method, which are all down first and then increasing, and the NMR method is not consistent with the above two: the $1/T_2^{XL}$ is increasing with the increase in CSDPF. This is because the $1/T_2^{XL}$ of NMR is only the characterization of crosslink degree in the vulcanization network; the tube model is more concerned with the crosslink situation of the rubber molecular chain on the surface of the filler. For the swelling method, the vulcanization network, the filler–rubber interaction and the filler–filler interaction are included [11]. The emphasis of the three methods is different; studying the structure of the rubber network from different angles is conducive to understanding the structure of the rubber network deeply.

4. Conclusions

CSDPF/NR vulcanizate was prepared by mechanical blending and the effects of CSDPF on the filler–rubber interaction and structure of rubber networks were studied. With an increase in CSDPF, the filler–rubber interaction in the compound increases. CSDPF can promote the formation of poly-sulfidic crosslinks in rubber vulcanization networks. Furthermore, the molecular chain movement ability of vulcanizates decreases and the crosslink density of vulcanizates increases, while the chemical crosslink and physical crosslink in vulcanization networks increase gradually.

Author Contributions: Experiments and original draft preparation, J.W.; review and editing, H.J. All authors have read and agreed to the published version of the manuscript.

Funding: The authors gratefully acknowledge the support from the Scientific Foundation of the Liming Vocational University (grant no. LZB202101, LMTD 202103, LMPT 202101).

Institutional Review Board Statement: Not applicable.

Informed Consent Statement: Not applicable.

Data Availability Statement: Correspondence and requests for materials should be addressed to J.W.

Conflicts of Interest: The authors declare no conflict of interest.

Abbreviations

CSDPF	Carbon–silica dual-phase filler
NR	Natural rubber
ZnO	Zinc oxide
RD	Poly(1,2-dihydro–2,2,4-trimethyl-quinoline)
NS	N-tert-Butyl-2-benzothiazolesulfenamide
XLD	Crosslink density
NMR	Nuclear magnetic resonance
MAS	Magic-angle spin
T_2	Spin–spin relaxation time
CPMG	Carr–Purcell–Meiboom–Gill
BdR	Bound rubber
G_c	Contribution of chemical crosslink to the elastic modulus
G_e	Contribution of physical crosslink to the elastic modulus

References

1. Scotti, R.; Wahba, L.; Crippa, M.; D'Arienzo, M.; Donetti, R.; Santo, N.; Morazzoni, F. Rubber-silica nanocomposites obtained by in situ sol-gel method: Particle shape influence on the filler-filler and filler-rubber interactions. *Soft Matter* **2012**, *8*, 2131–2143. [[CrossRef](#)]
2. Wang, M.J. The Role of Filler Networking in Dynamic Properties of Filled Rubber. *Rubber Chem. Technol.* **1999**, *72*, 430–448. [[CrossRef](#)]
3. Wang, M.J.; Lu, S.X.; Mahmud, K. Carbon–silica dual-phase filler, a new-generation reinforcing agent for rubber. Part VI. Time-temperature superposition of dynamic properties of carbon–silica-dual-phase-filler-filled vulcanizates. *J. Polym. Sci. Part B Polym. Phys.* **2000**, *38*, 1240–1249. [[CrossRef](#)]
4. Zhang, P.; Wang, M.-J.; Kutsovsky, Y.; Laube, S.; Mahmud, K. *A New Generation Carbon-Silica Dual Phase Filler (Csdpf) Part II. Application to Passenger Tread Compounds for Improved Tradeoff Among Rolling Resistance, Wet Traction and Treadwear Performance*; Meeting of Rubber Division, ACS: Cleveland, OH, USA, 2001.
5. Xiong, X.; Wang, J.Y.; Jia, H.B.; Ding, L.F.; Dai, X.; Fei, X. Synergistic effect of carbon black and carbon–silica dual phase filler in natural rubber matrix. *Polym. Compos.* **2014**, *35*, 1466–1472. [[CrossRef](#)]
6. Donnet, J.B. Reinforcement of Elastomers by Particulate Fillers. In *The Science and Technology of Rubber*; Mark, J.E., Erman, B., Roland, M., Eds.; Academic Press: Burlington, MA, USA, 2005; pp. 367–400.
7. Vidal, A.; Haidar, B. Filled Elastomers: Characteristics and Properties of Interfaces and Interphases, and Their Role in Reinforcement Processes. *Soft Mater.* **2007**, *5*, 155–167. [[CrossRef](#)]
8. Woff, S.; Wang, M.-J. Carbon Black Reinforcement of Elastomers. In *Carbon Black: Science and Technology*; Donnet, J.-B., Ed.; CRC Press: London, UK, 1993; pp. 289–356.
9. Litvinov, V.M.; Orza, R.A.; Klüppel, M.; van Duin, M.; Magusin, P.C.M.M. Rubber—Filler Interactions and Network Structure in Relation to Stress–Strain Behavior of Vulcanized, Carbon Black Filled EPDM. *Macromolecules* **2011**, *44*, 4887–4900. [[CrossRef](#)]
10. Wang, M.-J.; Zhang, P.; Mahmud, K. Carbon—Silica Dual Phase Filler, a new Generation Reinforcing Agent for Rubber: Part IX. Application to Truck Tire Tread Compound. *Rubber Chem. Technol.* **2001**, *74*, 124–137. [[CrossRef](#)]
11. Saatchi, M.M.; Shojaei, A. Effect of carbon-based nanoparticles on the cure characteristics and network structure of styrene–butadiene rubber vulcanizate. *Polym. Int.* **2012**, *61*, 664–672. [[CrossRef](#)]
12. Koenig, J.L. Spectroscopic Characterization of the Molecular Structure of Elastomeric Networks. *Rubber Chem. Technol.* **2000**, *73*, 385–404. [[CrossRef](#)]
13. Heinrich, G.; Vilgis, T.A. Contribution of entanglements to the mechanical properties of carbon black-filled polymer networks. *Macromolecules* **1993**, *26*, 1109–1119. [[CrossRef](#)]
14. Bokobza, L. The Reinforcement of Elastomeric Networks by Fillers. *Macromol. Mater. Eng.* **2004**, *289*, 607–621. [[CrossRef](#)]
15. Joly, S.; Garnaud, G.; Ollitrault, R.; Bokobza, L.; Mark, J.E. Organically Modified Layered Silicates as Reinforcing Fillers for Natural Rubber. *Chem. Mater.* **2002**, *14*, 4202–4208. [[CrossRef](#)]
16. Flory, P.J. Effects of Molecular Structure on Physical Properties of Butyl Rubber. *Ind. Eng. Chem.* **1946**, *38*, 417–436. [[CrossRef](#)]
17. Lin, W.; Bian, M.; Yang, G.; Chen, Q. Strain-induced crystallization of natural rubber as studied by high-resolution solid-state ^{13}C NMR spectroscopy. *Polymer* **2004**, *45*, 4939–4943. [[CrossRef](#)]
18. Varghese, T.V.; Ajith Kumar, H.; Anitha, S.; Ratheesh, S.; Rajeev, R.S.; Lakshmana Rao, V. Reinforcement of acrylonitrile butadiene rubber using pristine few layer graphene and its hybrid fillers. *Carbon* **2013**, *61*, 476–486. [[CrossRef](#)]
19. Wolff, S.; Wang, M.-J.; Tan, E.-H. Filler-Elastomer Interactions. Part VII. Study on Bound Rubber. *Rubber Chem. Technol.* **1993**, *66*, 163–177. [[CrossRef](#)]

20. Orza, R.A.; Magusin, P.C.M.M.; Litvinov, V.M.; van Duin, M.; Michels, M.A.J. Solid-State ^1H NMR Study on Chemical Cross-Links, Chain Entanglements, and Network Heterogeneity in Peroxide-Cured EPDM Rubbers. *Macromolecules* **2007**, *40*, 8999–9008. [[CrossRef](#)]
21. Orza, R.A.; Magusin, P.C.M.M.; Litvinov, V.M.; van Duin, M.; Michels, M.A.J. Network Density and Diene Conversion in Peroxide-Cured Gumstock EPDM Rubbers. A Solid-State NMR Study. *Macromol. Symp.* **2005**, *230*, 144–148. [[CrossRef](#)]